

Testing of metadielectric materials by non-contact corona charge deposition and Kelvin probe voltage measurement

1. INTRODUCTION

Linear capacitors are characterized by their *capacitance*, the ratio between the stored charge and the applied voltage. Capacitance is determined by the geometry and the permittivity of the dielectric material. If the dielectric material is highly nonlinear the concept of permittivity is not applicable, and one must introduce a new expression to compare the performance of various dielectrics. It is natural that such quantity would be the stored energy, in a general case defined as:

$$W = \int_0^{Q_f} V(Q) dQ \quad (1)$$

where Q is the total of free charges in the system. Free charges are introduced slowly from zero to Q_f and the molecules are polarized with the creation of bound charges. However, molecules are kept at equilibrium by means of stretching and twisting of the bonds, so only the free charges are included in Eq. (1). For the linear case, when $V = Q/C$, Eq. (1) reduces to a well-known expression:

$$W = Q_f^2 / 2C \quad (2)$$

To compare the resulting stored energy to currently available commercial devices, it is convenient to express it as specific energy measured in Watt hours per kilogram, as:

$$\frac{W}{M} \left(\frac{Wh}{kg} \right) = \int_0^{Q_f} V(Q) dQ / 3600 A d \rho \quad (3)$$

where A is the area of the electrodes, d is their separation, and ρ is the mass density of the dielectric material.

2. EXPERIMENTAL PROCEDURE

The setup of the corona charge deposition method is shown in Figure. 1. Our measurement device consists of the corona bar which induces the electric breakdown of surrounding gas

molecules and directs the positive or negative ions toward the thin film surface; the ampere

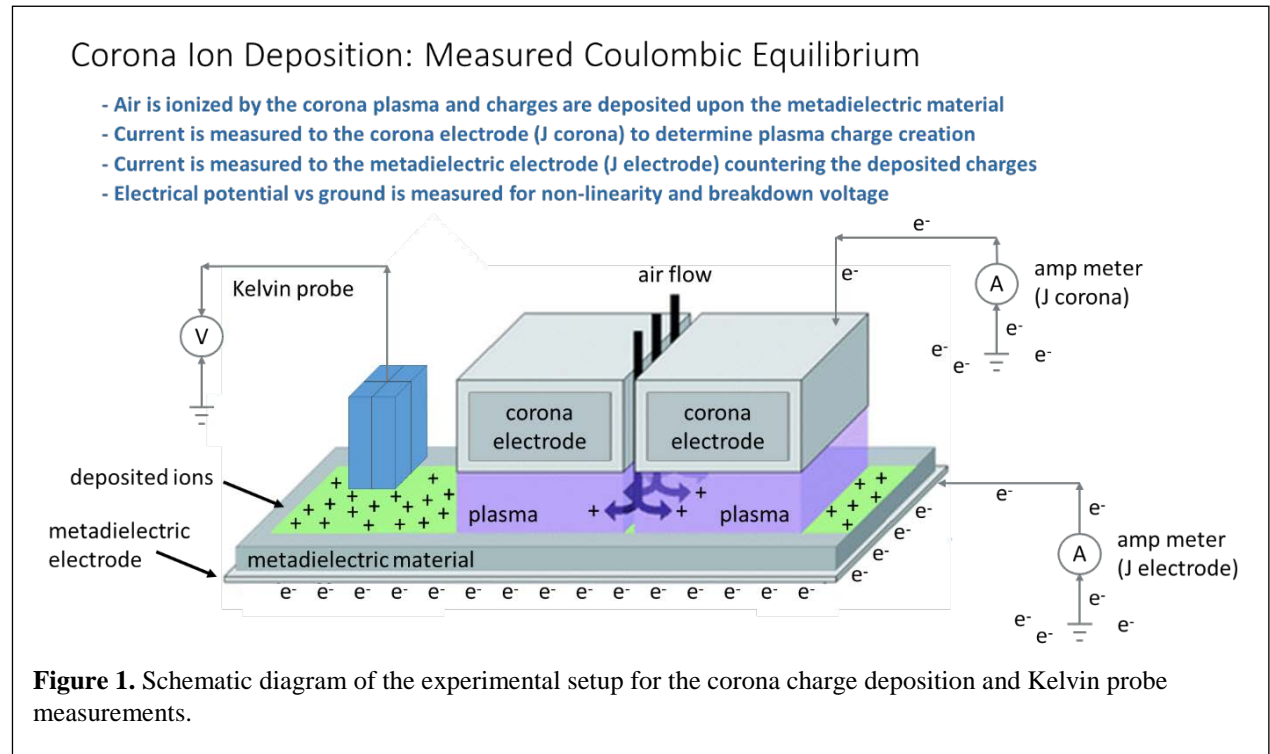


Figure 1. Schematic diagram of the experimental setup for the corona charge deposition and Kelvin probe measurements.

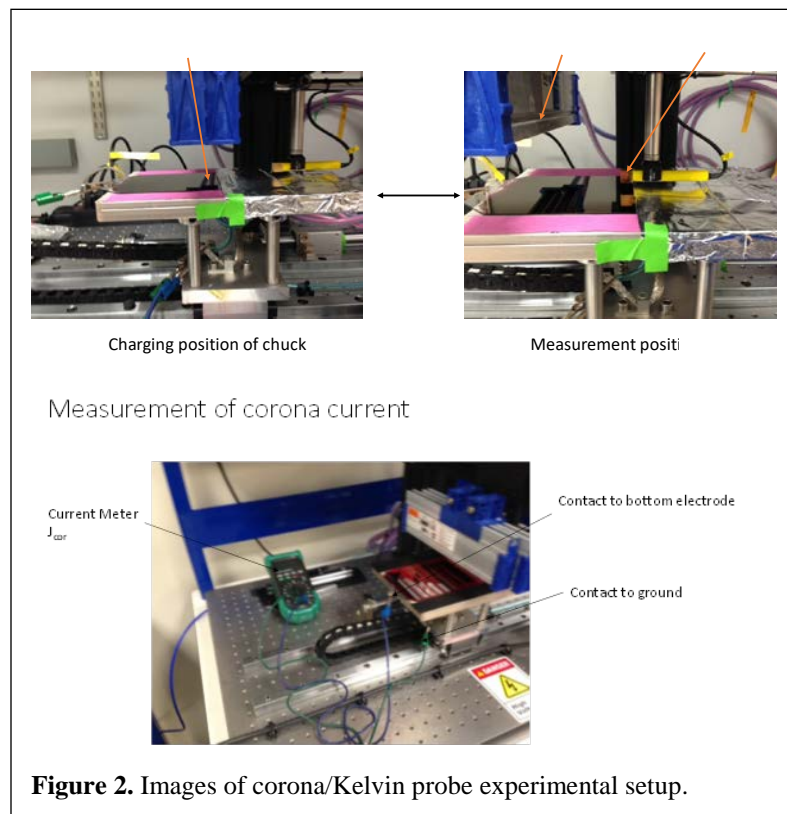


Figure 2. Images of corona/Kelvin probe experimental setup.

meter which measures the bottom electrode current corresponding to the opposite charge of the deposited ions; and the Kelvin probe apparatus which measures the surface potential with the respect to the ground. The images of actual apparatus are shown in Figure 2.

Corona charge deposition produces a layer of ions that are absorbed on the top surface, or within a few angstroms of the top surface of the dielectric material.

Lateral mobility of the ions is negligible as the diffusion coefficients of major ions are in 10^{-16} to 10^{-18} cm/sec. Deposition of ions is controlled by the potential difference between the corona bar and ground. This allows selective deposition of negative and positive ions from the ionized air. Absorbed ions on the top surface create a virtual top electrode upon the dielectric material. The bottom electrode is insulated from the virtual top electrode by the dielectric layer under investigation. **The virtual top electrode, dielectric material and bottom electrode form a capacitor.** The charges deposited on the top surface create a potential between the surface of the dielectric material and the bottom electrode which is connected to the ground. This potential is brought into coulombic equilibrium as charges from the ground are accumulated on the bottom. The current J_c producing the counter-charges is measured by an ampere meter between the ground and bottom electrode. Correspondingly, the total charge and the total charge density at the top surface of this film are given by,

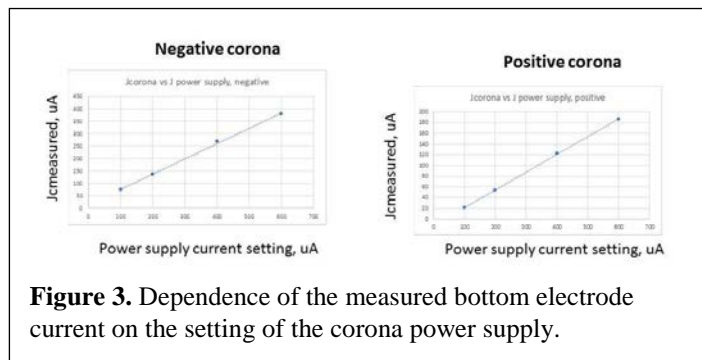
$$Q = J_c t \quad (4)$$

and

$$\sigma = J_c t / A, \quad (5)$$

respectively.

To validate this approach, we measure the dependence of the bottom electrode current, J_c , on

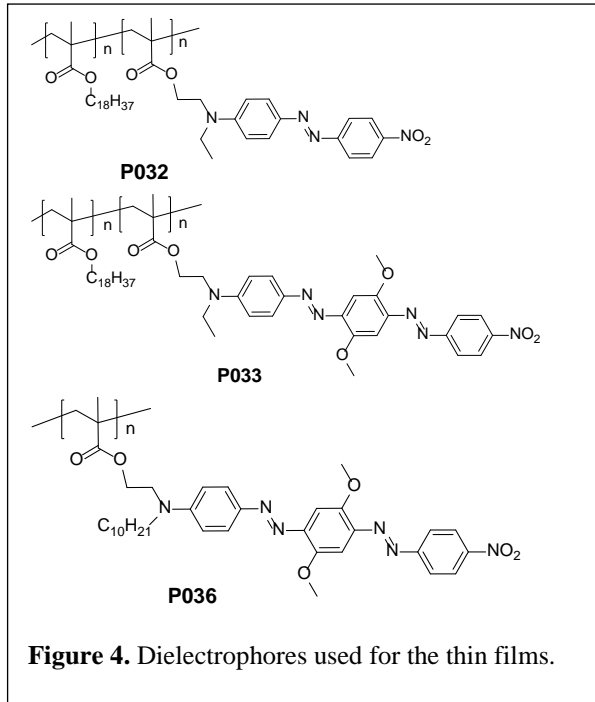


the power supply current setting of the corona system. The results are shown in Figure 3 and the obtained dependence is that of a straight line, i.e. the measured values of J_c indeed represent the amount of charges deposited on the top film surface. One can see that for

positive and negative coronas, J_c are different. This can be explained on the basis of the physical processes involved. For positive corona, the electrons are *collected* from the air in the region nearby the corona bar and all the processes happen in the gas without the involvement of the bar itself. For the negative corona, the electrons are *emitted* by the bar, so its material properties become important. It must be emphasized that these calibration lines are the same for all of the measured films, so the current from the bottom electrode depends on the amount of deposited charge only, not on the material properties.

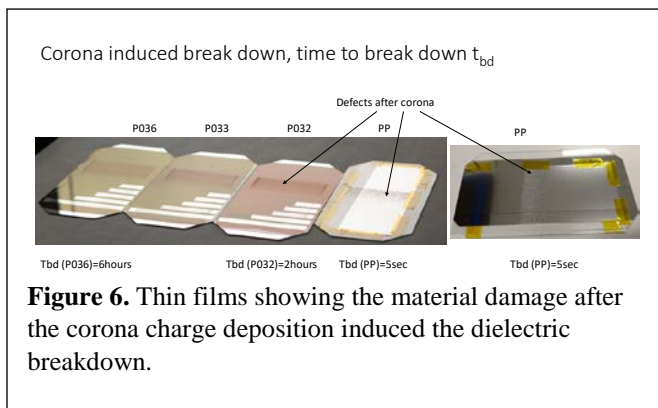
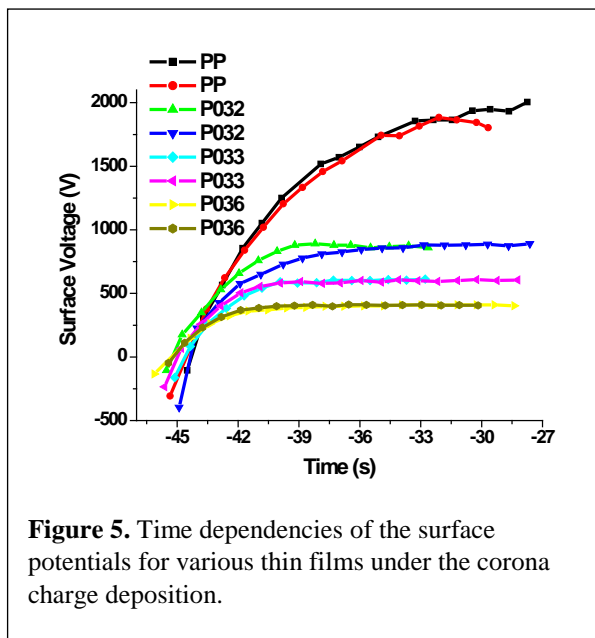
3. EXPERIMENTAL RESULTS

We present here the results of the measurements of organic thin films based on the dielectrophores units shown in Figure 4. For comparison, the polypropylene thin film was also



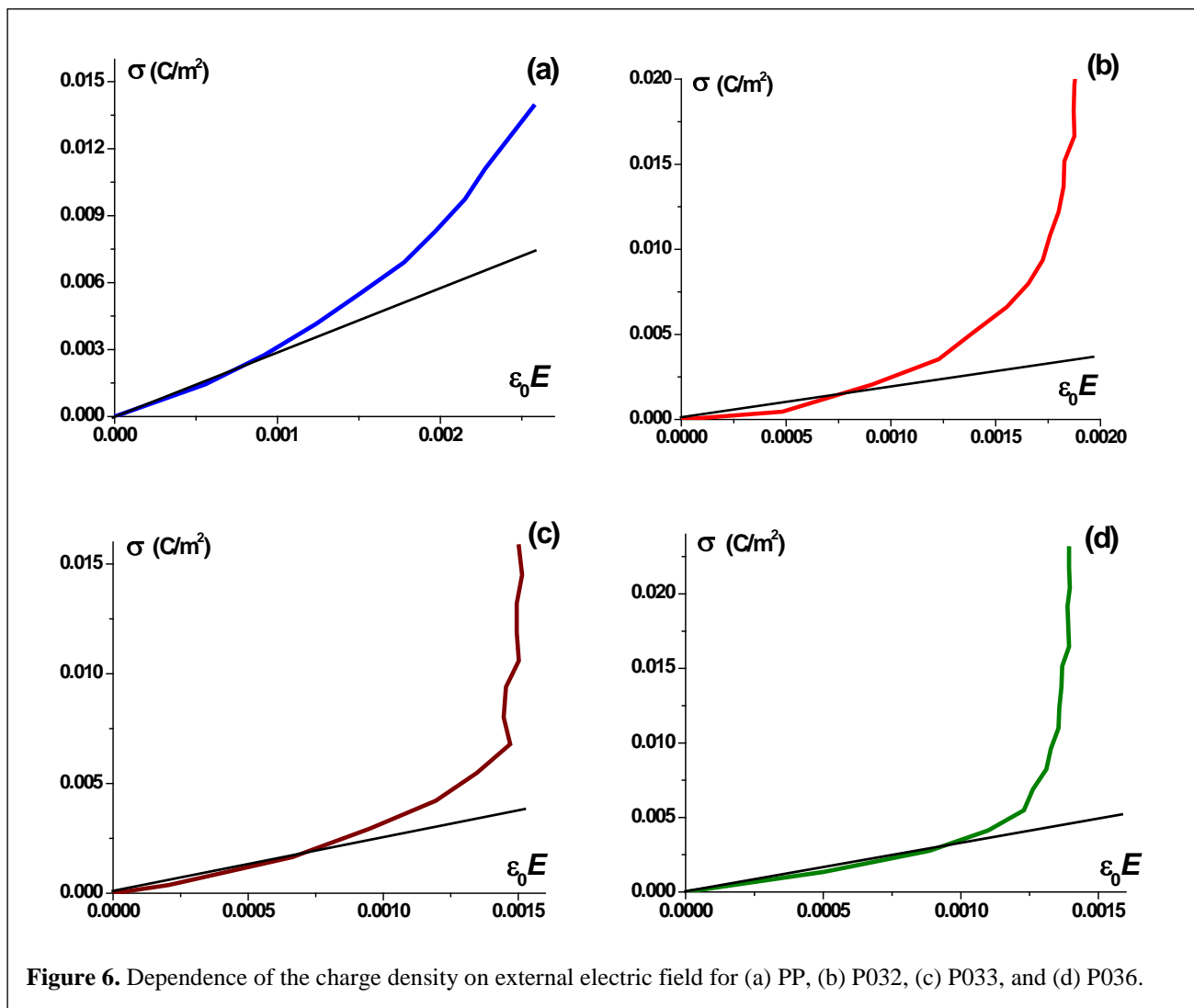
measured. The raw data, the time dependencies of the surface potentials for polypropylene (PP) film, P032, P033, and P036 films are shown in Figure 5 for the bottom electrode current of 5 to 10 A.

All the films were initially negatively charged and then were subjected to positive corona charge deposition. It is evident that for dielectrophores films (P032, P033, and P036), the surface potential saturates at decreasing voltage, while PP films exhibit electric breakdown after several seconds. The dielectrophores films remain intact during charge deposition for a much longer time than polypropylene before electric breakdown (2, 5, and 6 hours for P032, P033, and P036, respectively). After breakdown occurs, mechanical damage to the films is visible, as demonstrated in Figure 6.



4. EVALUATION OF EXPERIMENTAL DATA: LOW-FIELD DIELECTRIC CONSTANT

The initial linear region of Figure 5 can be used to estimate low-field dielectric constants, defined as $\epsilon = D / \epsilon_0 E = \sigma / \epsilon_0 E$, because according to the Gauss theorem, the electric displacement D is equal to the charge density σ . The external field E can be calculated as a ratio of the surface voltage and the film thickness. The charge density is related to the corona exposition time via Equation (5), where the surface area is $11.5 \times 6 \text{ cm}^2$. Correspondingly, Figure 5 can be replotted as the dependence of charge density on the external electric field, and the low-field dielectric constant can be calculated, as shown in Figure 6 and Table 1.



Structure	Thickness, μm	Low-field permittivity, ϵ	Calculated polarizability, α	Density of polarizable cores
PP	6	2.9	240	$26.1 \cdot 10^{26} \text{ m}^{-3}$
P032	4.1565	2.1	428	$10.2 \cdot 10^{26} \text{ m}^{-3}$
P033	3.56	2.4	888	$5.7 \cdot 10^{26} \text{ m}^{-3}$
P036	2.5985	3.2	888	$7.6 \cdot 10^{26} \text{ m}^{-3}$

Table 1. Parameters of thin films and dielectrophores units.

5. EVALUATION OF EXPERIMENTAL DATA: DENSITY OF POLARIZABLE CORES

The obtained values of dielectric constants at the linear regime can help us to estimate the density of the polarizable cores. The macroscopic polarization is given by

$$P = Np_{ind}, \quad (6)$$

where p_{ind} is the induced dipole and N is the density of the dipoles.

The induced dipole in the linear regime can be expressed in terms of the local field as

$$p_{ind} = \alpha E_{loc}, \quad (7)$$

where α ($= \alpha_{xx}$) is the polarizability, and the local field has the Lorentz form

$$E_{loc} = E + \frac{P}{3\epsilon_0}. \quad (8)$$

Combining Equations 6-8 leads to the usual Clausius–Mossotti relation,

$$\frac{(\epsilon - 1)}{(\epsilon + 2)} = \frac{N\alpha}{3\epsilon_0}, \quad (9)$$

and the dipole density can be estimated as

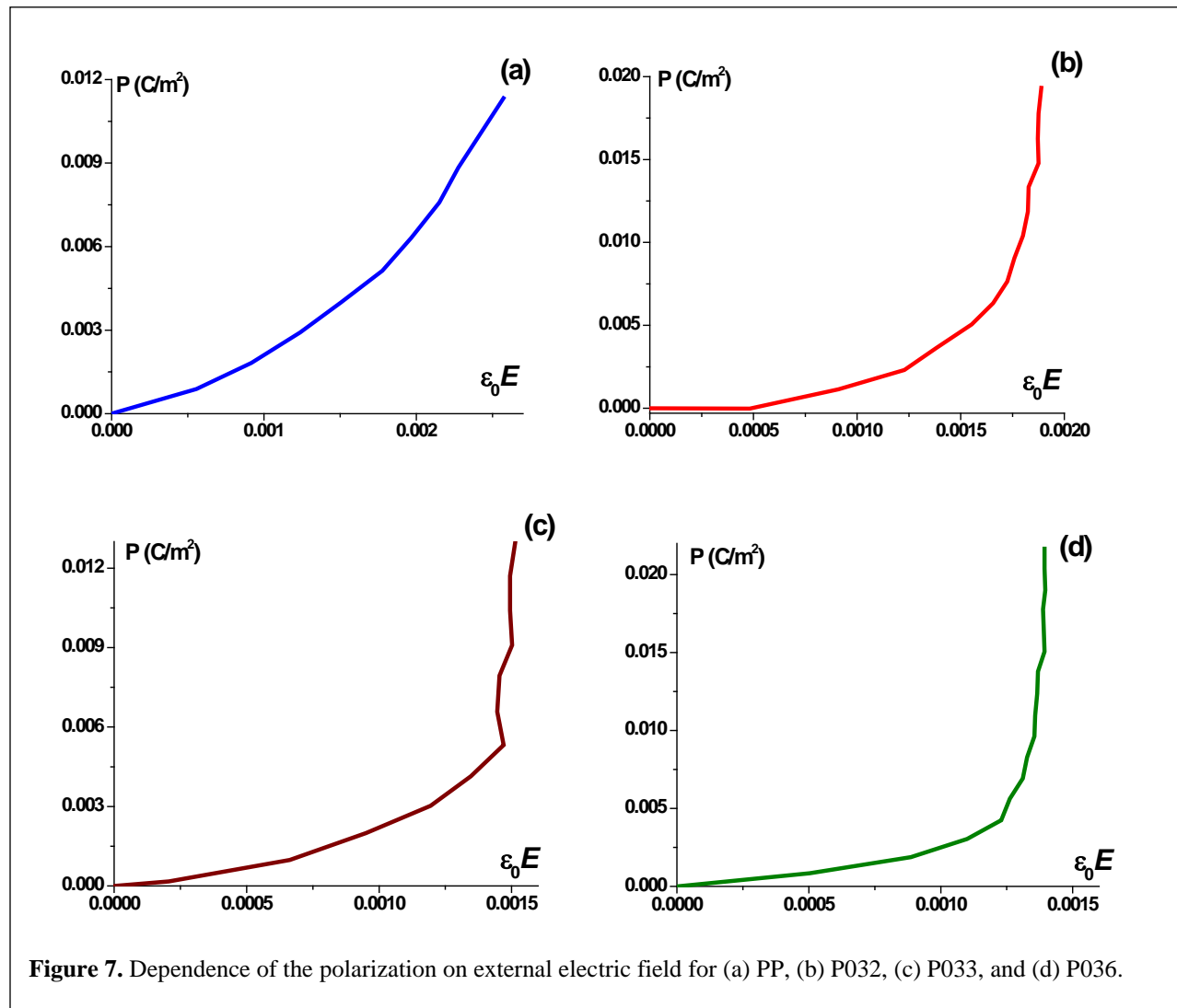
$$N = \frac{3\epsilon_0}{\alpha} \frac{(\epsilon - 1)}{(\epsilon + 2)}, \quad (10)$$

where α is expressed in atomic units, $1 \text{ a.u.} = e^2 a_0^2 / E_h$, e is the electron charge, a_0 is the Bohr radius, and E_h is the Hartree energy.

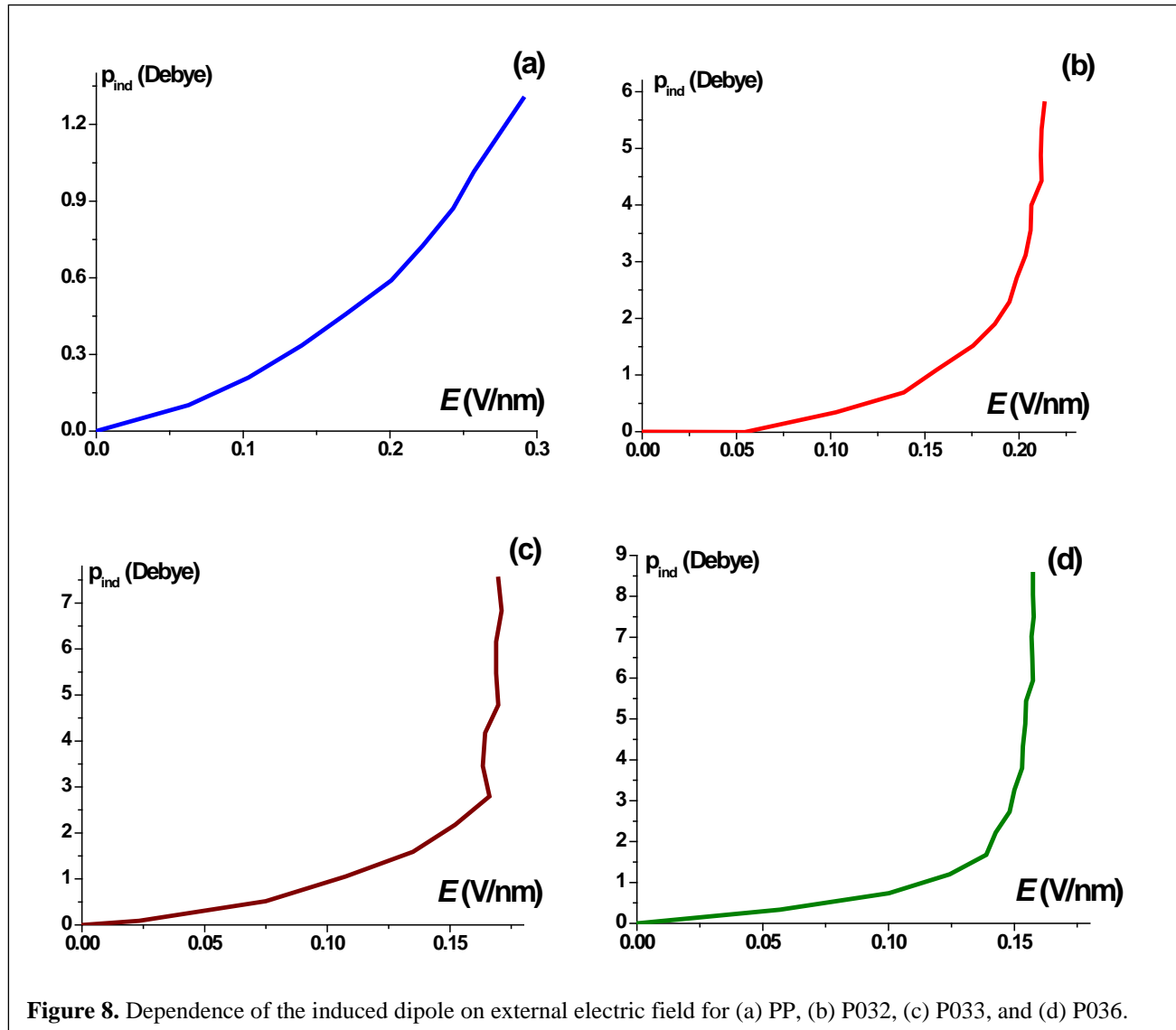
The polarizability α can be obtained from quantum chemistry calculations using the Gaussian 09 software and the results are presented in Table 1 jointly with the dipole density values calculated using Equation 10. One can see that the dipole density for the polypropylene film is quite large and it compensates for its relatively small polarizability. For dielectrophores, the dipole density is smaller because significant regions of the films are occupied by the resistive tails. The smaller size of the polarizable core of P032 results in a higher dipole density. The polarizable cores of P033 and P036 are the same and the difference of the low-field permittivity is explained by higher dipole density of P036.

6. EXPERIMENTAL DATA: POLARIZATION AND INDUCED DIPOLES

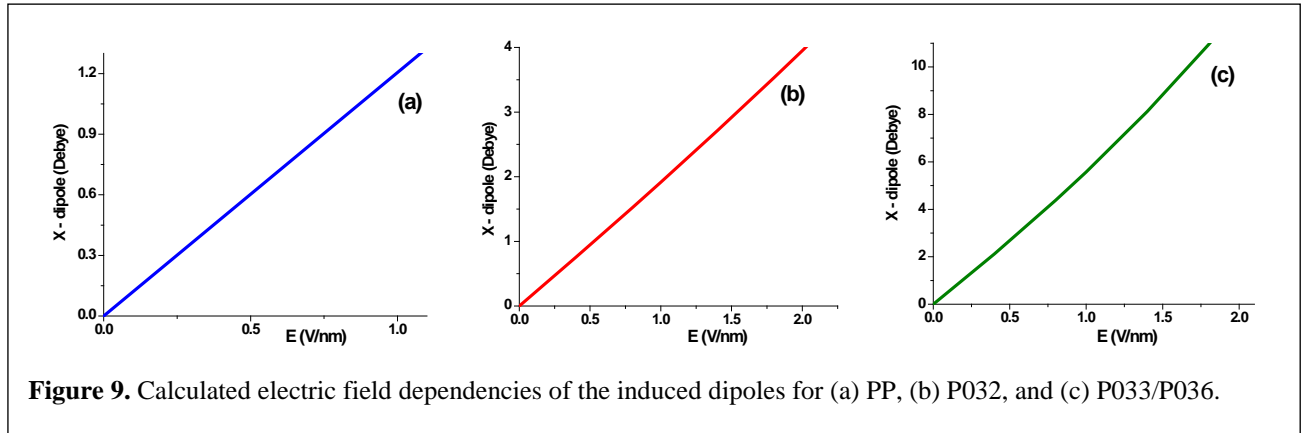
Dependence of the polarization on the external electric field can be obtained from Figure 5 and equation $\sigma = P + \epsilon_0 E$. The results for the PP and dielectrophores films are shown in Figure 7.



These graphs can be used to determine the experimental dependence of the induced single-molecule dipole upon the external electric field using Equation 3. The results are presented in Figure 8 with dipoles shown in Debye units ($1 \text{ Debye} = 3.33564 \cdot 10^{-30} \text{ C m}$). For future comparison with the results obtained in calculations, the field is shown in V/nm.

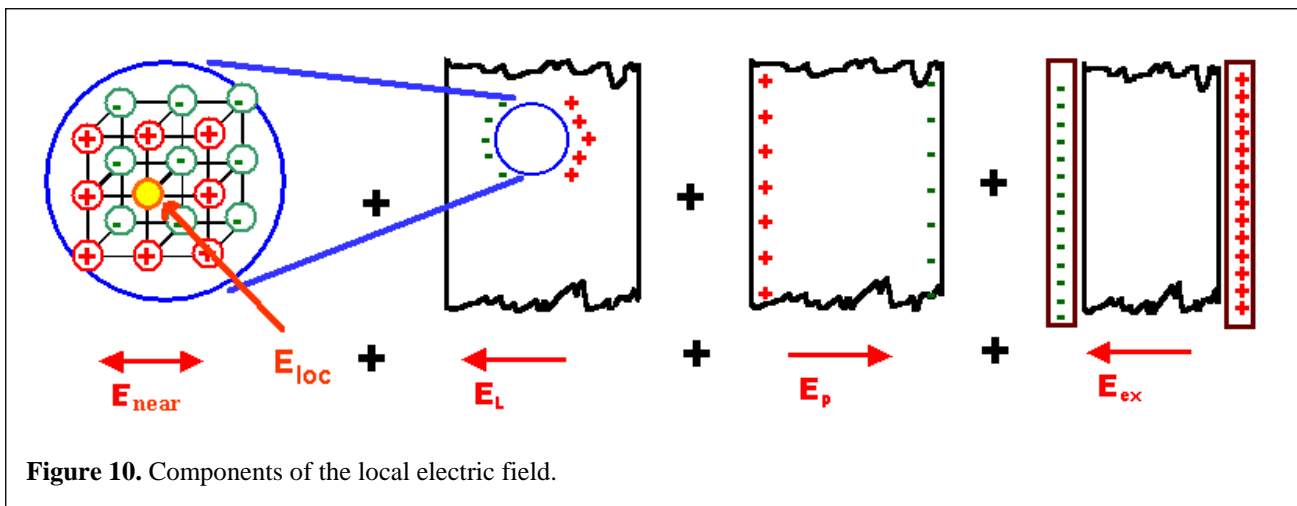


The calculated electric field dependencies of the induced dipoles are shown in Figure 9. One can see that these dependencies are completely linear and all of the nonlinearities obtained experimentally are not the properties of single molecules but come from the crystalline structures which create local fields similar to Equation 8.



7. LOCAL FIELD IN DIELECTRICS

Local field involved in Equation 8 can be understood from the following approximate consideration, called Lorentz approach, see Figure 10.



In this approach we decompose the total field into four components. Let us imagine that we remove a small volume containing a few atoms from the material. We want to know the local field in the center of this volume while it is still in the material. We define that field by the force it exerts on a charge at the center of the sphere that acts as a "probe". The essential trick is to calculate the field produced from the atoms inside the volume and the field inside the now empty volume in the material. The total local field then is simple the sum of both. We do not consider the charge of the "probe" in computing the field that it probes. The cut-out volume must not contain the charge we use as the field probe. The cut-out material, in general, could produce an

electrical field at its center since it is composed of charges. This is the 1st component of the field, E_{near} , which takes into account the contributions of the atoms or ions inside the volume. We will consider that field in an approximation where we average over the volume of the small volume. E_{near} , however, is not the only field that acts on our probe. We must include the field that all the other atoms of the crystal produce in the hollow volume left after we cut out some material. This field now fills the "empty" void left by removing the volume of dielectric material. This field is called E_L (the "L" stands for Lorentz); it compensates for the cut-out part - and that provides our 2nd component. Now we only need to add the "macroscopic" field from the polarization of the material and the charges on electrodes, $E = (\sigma - P)/\epsilon_0$.

$E_{near} = 0$ for isotropic materials, and while the dielectrophores films are not isotropic, we neglect this field as a first approximation. From Figure 10 it is evident that the Lorentz field is proportional to the polarization, $E_L = LP/\epsilon_0$, where L is the Lorentz factor depending on the geometry and having a value between 0 and 1. It can be calculated for simple shapes of our removed volume. In particular, for a sphere $L = 1/3$, leading to Equation 9. For the general case, the local field has the form:

$$E_{loc} = E + L \frac{P}{\epsilon_0}. \quad (11)$$

Combining Equations 6, 7 and 11 for arbitrary L , we obtain:

$$\epsilon_0 E = P \left(\frac{\epsilon_0}{N\alpha} - L \right), \quad (12)$$

and the derivative of the electric field with respect to polarization equals to zero when

$$L - \frac{\epsilon_0}{N\alpha} = L - \frac{537.6}{n\alpha} = 0, \quad (13)$$

where n is the dipole density in 10^{-27} m^{-3} or can even be negative. For high n and α , Equation 13 can be satisfied, and the dependence of polarization on the electric field looks like the corona experiment, see Figure 7. There can be two reasons for the tuning of the system into the condition of Equation 13. First, if the system is nonlinear, this nonlinearity can be included into the field dependence of α . **However, even if the system is linear, as can be seen from Figure 9, the application of electric field in soft matter can lead to the changing of the geometry and, consequently, to the tuning of L .**

8. EVALUATION OF EXPERIMENTAL DATA: STORED ENERGY DENSITY

To make qualitative estimations, we replot Figure 5 as a dependence of the surface potential on

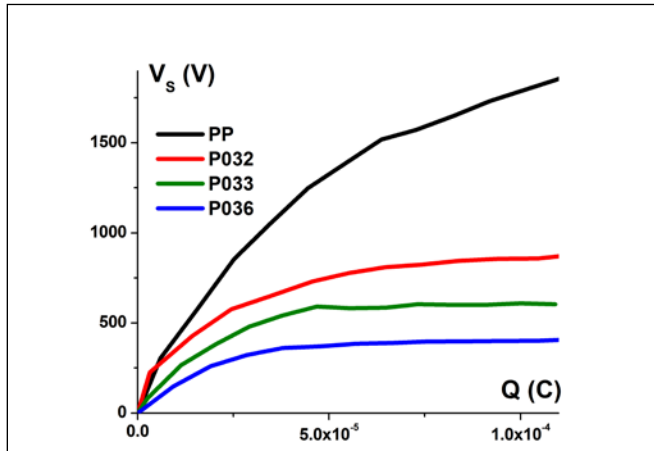


Figure 11. Dependence of the surface potential on the total deposited corona charge for various dielectrophores in comparison to the polypropylene film.

the total deposited charge, see Figure 11, and use Equation 3 to determine the stored specific energy for our thin films. The integrals can be calculated numerically, and the specific energy can be evaluated for the films with areas of $11.5 \times 6 \text{ cm}^2$ when they are charged up to the breakdown. The mass density for all the materials is about 1000 kg/m^3 . The thicknesses, maximal surface potentials, the films breakdown times, and the obtained energy densities are presented in Table 2. One can see that the stored specific energies for our dielectrophores are several orders of the magnitude larger than that of the PP film. Moreover, as the current generation of the batteries has specific energies of approximately 250-Watt hours per kilogram, the dielectrophore-based capacitors would have far greater specific energy than lithium ion batteries, while also being superior in all other properties.

	d (μm)	Vs (V)	t _{bd} (hours)	W/M (Wh/kg)
PP	6	1856	0.003	0.9
P032	4.1565	880	2	614
P033	3.56	609	5	1226
P036	2.5985	404	6	1353

Table 1. Estimations of the stored energy density.